J. Biochem. 131, 679–685 (2002)

Structure of External Aldimine of *Escherichia coli* CsdB, an IscS/NifS Homolog: Implications for Its Specificity toward Selenocysteine[1]

Hisaaki Mihara, Tomomi Fujii, Shin-ichiro Kato, Tatsuo Kurihara, Yasuo Hata, and Nobuyoshi Esaki[2]

Institute for Chemical Research, Kyoto University, Uji, Kyoto 611-0011

Received January 25, 2002; accepted February 21, 2002

***Escherichia coli* CsdB is a pyridoxal 5′-phosphate (PLP)–dependent enzyme that catalyzes both cysteine desulfuration and selenocysteine deselenation. The enzyme has a high specific activity for L-selenocysteine relative to L-cysteine. On the other hand, its paralog, IscS, exhibits higher activity for L-cysteine, which acts as a sulfur donor during the biosynthesis of the iron-sulfur cluster and 4-thiouridine. The structure of CsdB complexed with L-propargylglycine was determined by X-ray crystallography at 2.8 Å resolution. The overall polypeptide fold of the complex is similar to that of the uncomplexed enzyme, indicating that no significant structural change occurs upon formation of the complex. In the complex, propargylglycine forms a Schiff base with PLP, providing the features of the external aldimine formed in the active site. The Cys364 residue, which is essential for the activity of CsdB toward L-cysteine but not toward L-selenocysteine, is clearly visible on a loop of the extended lobe (Thr362–Arg375) in all enzyme forms studied, in contrast to the corresponding disordered loop (Ser321–Arg332) of the *Thermotoga maritima* NifS-like protein, which is closely related to IscS. The extended lobe of CsdB has an 11-residue deletion compared with that of the NifS-like protein. These facts suggest that the restricted flexibility of the Cys364-anchoring extended lobe in CsdB may be responsible for the ability of the enzyme to discriminate between selenium and sulfur.**

Key words: crystal structure, cysteine desulfurase, NifS, pyridoxal 5′-phosphate, selenocysteine lyase.

Cysteine desulfurases and selenocysteine lyases both catalyze the same type of reaction: the desulfuration of L-cysteine to S^0 and L-alanine (*1*) and the deselenation of L-selenocysteine to Se^0 and L-alanine (*2*), respectively.

Cysteine desulfurases such as NifS and IscS act on both L-cysteine and L-selenocysteine, although the physiological role of the enzyme is to supply sulfur atoms for the biosynthesis of iron-sulfur clusters (*3, 4*), 4-thiouridine (*5*), and thiamin (*6*). NifS from a nitrogen-fixing bacterium was originally reported by Zheng *et al.* as an enzyme required for the maintenance or formation of iron-sulfur clusters in nitrogenase (*1*). NifS orthologs found in a wide variety of non-nitrogen-fixing organisms, including *Escherichia coli,* are designated IscS for their proposed function in iron-sulfur cluster biosynthesis (*3*). Recent progress in this field has revealed the multiple roles of IscS as sulfur donors for biotin (*7*), thiamin (*6*), and 4-thiouridine in tRNA (*5*), in addition to iron-sulfur cluster (*4*). During the cysteine desulfuration catalyzed by IscS and NifS, the cysteine persulfide formed on a conserved active-site Cys residue is believed to mediate sulfur transfer (*8*).

In contrast to cysteine desulfurase, selenocysteine lyase is highly specific for L-selenocysteine. The activity of mammalian selenocysteine lyase toward L-cysteine is negligibly small. The selenocysteine lyase from pig liver is entirely specific for L-selenocysteine and does not act on L-cysteine (*2*). The recombinant selenocysteine lyase from mouse liver shows 6,700 times higher activity for L-selenocysteine than for L-cysteine (*9*). Thus, selenocysteine lyase has the ability to discriminate between two congeneric elements, selenium and sulfur, whereas many other enzymes acting on sulfur-containing compounds do not. There are a few examples of enzymes that are specific for a selenium-containing substrate (*10*), but the mechanism of such discrimination is poorly understood (for reviews, see Refs. *11–13*).

We have characterized CsdB from *E. coli* as an enzyme homologous to cysteine desulfurase and selenocysteine lyase (*14*). The amino acid sequence of CsdB exhibits about 20% identity with the sequences of *Azotobacter vinelandii* NifS and *E. coli* IscS. The specific activity of IscS for L-cysteine is higher than that of CsdB, while CsdB exhibits 290 times higher activity toward L-selenocysteine than toward

[1] This work was supported in part by a grant from the Rice Genome Project PR-2202, MAFF, Japan (to Y.H.), a Research Grant from the Japan Society for the Promotion of Science (Research for the Future) (to N.E.), Grants-in-Aid for Scientific Research 11480179 (to N.E.) and 11169220 (to Y.H.) from the Ministry of Education, Science, Sports, and Culture of Japan, and Grants-in-Aid for Scientific Research 13480192 (to N.E.) and 13033020 (to Y.H.), and a Grant-in-Aid for Scientific Research on Priority Areas (B) 13125203 (to N.E.) from the Ministry of Education, Culture, Sports, Science and Technology of Japan. The atomic coordinate and structure factor (code 1I29) have been deposited in the Protein Data Bank, Research Collaboratory for Structural Bioinformatics, Rutgers University, New Brunswick, NJ (http://www.rcsb.org/).

[2] To whom correspondence should be addressed. Tel: +81-774-38-3240, Fax: +81-774-38-3248, E-mail: esaki@scl.kyoto-u.ac.jp

Abbreviations: KPB, potassium phosphate buffer; PG, propargylglycine (2-amino-3-butynoic acid); PLP, pyridoxal 5′-phosphate.

L-cysteine. Thus, CsdB is functionally much closer to selenocysteine lyase than to cysteine desulfurase (*14*). In a previous study (*15*), we showed that the catalytic mechanisms of CsdB, IscS, and CSD (another paralog in *E. coli*) are similar to one another. A conserved Cys residue plays a critical role as a nucleophile attacking the sulfhydryl group of the substrate L-cysteine, whereas the residue is not essential for the deselenation of L-selenocysteine (Scheme 1). The corresponding active-residue in CsdB is Cys364.

We recently determined the structure of CsdB by X-ray crystallography (*16*). CsdB is a homodimer with a subunit molecular weight of 44,439. The overall fold of the CsdB subunit is similar to those of enzymes belonging to the α-family of PLP-dependent enzymes (*17, 18*). Each subunit consists of an N-terminal segment (residues 1–21) containing two α-helices, a small domain (residues 33–298) containing a four-stranded antiparallel β-sheet flanked by three α-helices, and a large domain (residues 22–32 and 299–406) of α/β-fold containing a seven-stranded β-sheet flanked by seven helices, with one molecule of PLP in aldimine linkage with Lys226. Residues 362–375 form a lobe extending from the small domain to the large domain of the subunit. The extended lobe contains the conserved Cys364 and constitutes one side of the entrance rim to the active site. The side chain of Cys364 is located near the γ-atom of a modeled substrate docked in the active site (*16*). However, details of the substrate-binding site are not known due to the structure determination of the substrate-free enzyme. In order to define the substrate-binding site and find the structural bases that enable CsdB to discriminate between selenium and sulfur in substrates, we solved the crystal structure of the enzyme complexed with a substrate analog, L-propargylglycine (PG, 2-amino-3-butynoic acid), and compared the structure with those of the uncomplexed CsdB and the *Thermotoga maritima* NifS homolog (tmNifS). tmNifS is closely related in amino acid sequence to *A. vinelandii* NifS and *E. coli* IscS, and its structure has recently been solved by Kaiser *et al.* (*19*). The comparison provided deeper insight into the substrate binding mode in CsdB and the difference in substrate specificity between CsdB and NifS/IscS. In this paper, we describe the crystal structure of CsdB complexed with L-propargylglycine and compare its structure with those of the uncomplexed CsdB and tmNifS. This is the first report of the external aldimine structure of an IscS/NifS homolog.

EXPERIMENTAL PROCEDURES

Preparation of Crystals—*E. coli* CsdB was expressed and purified as described previously (*14*). The enzyme was stored at a concentration of 20 mg/ml in 10 mM KPB (pH 7.4). Crystals of CsdB were grown at 25°C using the hanging drop vapor diffusion method of enzyme droplets against a reservoir solution (0.1 M KPB, 1.4 M sodium acetate, pH 6.8). The droplet was prepared by mixing 5 μl of enzyme solution and an equal volume of reservoir solution. The yellow and tetragonal-bipyramidal crystals of CsdB appeared in one day and grew to a typical size of 0.5 × 0.5 × 0.4 cm^3 within a couple of days. The space group of the CsdB crystals was $P4_32_12$ with unit cell dimensions of $a = b = 128.1$ Å and $c = 137.0$ Å. There was one subunit of CsdB in the asymmetric unit.

Crystals of CsdB complexed with PG were prepared at 25°C by soaking uncomplexed CsdB crystals in 0.1 M KPB (pH 6.8) containing 0.8 M PG and 2 M pyruvate for 1 day. Pyruvate was added to the soaking solution because it slightly enhances the activity of the enzyme (*15*), although X-ray analysis of the crystal soaked in 0.1 M KPB (pH 6.8) containing 0.8 M PG and 1.4 M sodium acetate produced an electron density map identical to that obtained with the solution containing pyruvate.

Data Collection and Processing—Diffraction data for the complex crystal were collected at 20°C with a Rigaku R-AXIS IIc imaging plate detector system using graphite-monochromated Cu*K*α radiation produced by a Rigaku RU-300 rotating anode X-ray generator operated at 40 kV and 100 mA. Data collection was performed with a crystal sealed in a glass capillary. The crystal-to-detector distance was set to 130.0 mm. The diffraction pattern of each 1.5° crystal oscillation was recorded in 15 min. Data processing was accomplished at 2.8 Å resolution with the R-AXIS IIc data processing software package. All the frames of the diffraction data were merged and scaled together into a set of unique reflection data. The statistics of data collection and processing are summarized in Table I.

Structure Determination and Refinement—The subunit structure of the CsdB complex was analyzed using the subunit structure of the uncomplexed CsdB containing the Phe3–Gly406 region of the 406-residue polypeptide as a starting model, which was previously reported at 2.8 Å resolution to an *R*-factor of 18.7% (PDB # 1C0N) (*16*). First, the protein subunit of the CsdB-PG complex dimer was appropriately positioned by a 3.5 Å rigid-body refinement using the program CNS (*20*). Further refinement of the structural model was carried out at 2.8 Å resolution with the simulated annealing protocol of CNS, followed by positional and individual temperature factor refinements with the isotropic overall *B*-factor and bulk solvent corrections. The regions of conformational changes were checked on the

TABLE I. **Statistics of data collection and refinement of CsdB complexed with L-propargylglycine:**

Data collection statistics	
Resolution (Å)	50–2.8
Observed reflections ($I > 1\sigma_I$)	65,095
Unique reflections ($I > 1\sigma_I$)	23,684
Completeness (%)	82.3
R_{merge}[a] (%)	9.63
Refinement statistics	
R-factor[b] (%) (last shell)	20.9 (42.1)
R_{free}[c] (%) (last shell)	23.3 (42.5)
Number of atoms	
Protein/PLP/Ligand	3,096/15/6
Mean *B*-factors (Å²)	
Main chain/Side chain	40.0/41.9
PLP/Ligand	32.3/37.9
rmsd bonds (Å)	0.006
rmsd angles (deg)	1.172
Ramachandran plot quality[d] (%)	
Most favored	89.2
Allowed	10.5
Disallowed	0.3

[a] $R_{merge} = \Sigma_i|I_i - \langle I_i\rangle|/\Sigma_i I_i$, where $\langle I_i\rangle$ is the average of I_i over all symmetry equivalents. [b] *R*-factor $= 100\Sigma||F_o| - |F_c||/\Sigma|F_o|$, where $|F_o|$ and $|F_c|$ are the observed and calculated structure factor amplitudes, respectively. [c] R_{free} = *R*-factor, which is calculated for a selected subset of the reflections (5%) excluded from the refinement. [d] Most favored, additional and generously allowed, and disallowed regions are defined by PROCHECK.

basis of the $2F_o$–F_c and F_o–F_c difference electron density maps and rebuilt manually with the program TurboFRODO (*21*). In the initial stage of refinement, the polypeptide structure was refined in the complex. Then, the model of PLP was fitted into the electron density and included in the subsequent refinements. In the final stage of refinement, the model of the ligand moiety was fitted into the electron density lump occurring near PLP in the $2F_o$–F_c omit map of the complex. The model of the ligand was modified to bond covalently to that of PLP at the appropriate position. The complex structure was further refined to convergence. The refinement statistics are summarized in Table I.

Site-Directed Mutagenesis—Mutations were introduced into pCSDB (*14*) to produce H123A and R379A by PCR according to the overlap extension method (*22*). The following mutagenic primers were used: 5′-CATGATTACGAGTTCAGGAGGTGC-3′ and 5′-TAAGCGTGGGCCTCCATCTG-3′ for H123A and 5′-CATGATTACGAGTTCAGGAGGTGC-3′ and 5′-AGCGACGCCGCGCACATCGC-3′ for R379A. To construct H55A, the QuikChange™ site-directed mutagenesis kit (Stratagene, La Jolla, CA) was employed using pCSDB as a template with primers 5′-GGCTACGCGGCGGTGGCTCGTGGTATTCATACC-3′ and 5′-GGTATGAATACCACGAGCCACCGCCGCGATGCC-3′. The activities of the mutant enzymes were measured using L-selenocysteine as a substrate (*14*) unless otherwise noted.

RESULTS AND DISCUSSION

Overall Structure—We have analyzed the structure of the CsdB-PG complex using a crystal soaked in solutions containing PG. PG was used as a substrate analog because it has a Cγ atom of an ethinyl moiety in place of the Seγ atom of selenocysteine. The Cγ atom is unlikely to be cleaved off, and, therefore, PG was expected to provide an intermediate complex with CsdB. The polypeptide backbone of the structure is complete except for the N-terminal Met1 residue, which is invisible on the electron density map. No clear electron density was found for the side chains of Ile2, Lys7, Arg56, Ile58, Glu63, and Lys341. Therefore, these residues are included in the final model as alanine. The structure has good geometry. The polypeptide dihedral angles (ϕ, ψ) for almost all residues fall in either the most favored or the additional allowed regions defined by the program PROCHECK (*23*). The overall structure of the complex is quite similar to that of the uncomplexed CsdB reported previously (*16*), with an average rms deviation of 0.25 Å over all Cα-atoms (Fig. 1). There are no differences in crystal packing, no significant conformational changes, and no global domain movements as compared with the uncomplexed structure. In the complex, the domain orientation in the subunit and the subunit arrangement in the dimer are the same as those of the uncomplexed CsdB. This implies that there is no subunit movement in the CsdB dimer upon substrate binding. The plots of rms Cα deviations of the CsdB-PG structure from that of CsdB show relatively large deviations in three regions, Val19–Asn20, His55–Ile58, and Gly251–Ser254, and small deviations around Arg136 and Leu339. Val19–Asn20, Arg136, and Leu339 are located on the surface of the molecule and are exposed to the solvent. Gly251–Ser254 contains the Gly-Gly-Gly triplet motif and is situated near the active site, possibly providing flexibility for the enzyme. The most remarkable region in the deviation is the loop containing His55–Ile58. This region extrudes to the β-substituent of the ligand. This large deviation seems to be caused by the high flexibility in the region of His55–Ile58.

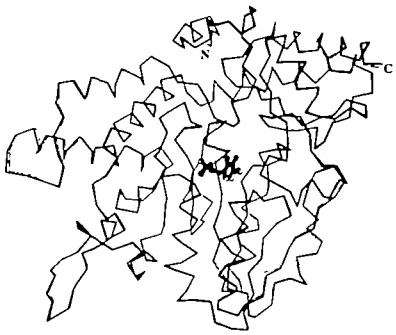

Fig. 1. **Superposition of the Cα trace of the CsdB-PG complex (thicker lines) on that of the uncomplexed CsdB (thinner lines).** The PLP moieties are depicted as ball-and-stick models. The figure was generated by MOLSCRIPT (*29*).

Active-Site Structure of the Propargylglycine-Complex Adopting an External Aldimine—Analyses of the F_o–F_c and $2F_o$–F_c omit maps for the crystal soaked in PG solution suggested that an additional electron density peak among PLP, Arg379, and His123 should be interpreted as a PG molecule (Fig. 2a). The observed density peak was not assigned to pyruvate because an electron density peak identical to that shown in Fig. 2a was obtained with the crystal soaked in PG solution without pyruvate (data not shown). The density is connected with that for C4′ of PLP, and there is no density peak linking PLP to Lys226, suggesting that PG is covalently bonded to PLP and that the side chain of Lys226 moves apart from PLP. Although the electron density corresponding to Cγ of PG is relatively ambiguous, the Cβ-Cγ bond is unlikely to be cleaved by CsdB. In addition, our biochemical analysis showed that CsdB does not utilize PG as a substrate or as an irreversible inhibitor (data not shown). Therefore, the complexed CsdB structure was modeled as the external aldimine with PG. Except for Cγ, the model of PG fits into the observed density (Fig. 2a). PG is placed in the active site by the hydrogen bond between the α-carboxyl group of PG and the guanidino group of Arg379 with a distance of 3.1 Å. Multiple residues interact with the PLP moiety of the external aldimine in the PG complex. The OP2 atom of PLP is hydrogen-bonded to the side-chain Oγ and the main-chain N atoms of Thr95. The OP3 atom is hydrogen-bonded to the side-chain Oγ atom of Ser223 and the side-chain Nε2 atom of His225. The OP1 atom is hydrogen-bonded to the side-chain Oγ and the main-chain N atoms of Thr278* in the other subunit. These binding modes of the phosphate group of PLP in the complex are similar to those of the uncomplexed CsdB. Asp200 in the complex forms a hydrogen bond with the pyridine nitrogen atom N1 of PLP in the same manner as in the uncomplexed structure (Fig. 2b).

Some changes in PLP binding and side-chain conformation of the polypeptide are observed upon formation of the PG complex. Figure 3 shows the active site of the CsdB-PG complex superimposed on that of the uncomplexed CsdB. In the CsdB-PG complex, the α-carboxyl group of PG is

hydrogen-bonded to the Nη2 atom of Arg379 (Fig. 2b). The conformation of Arg359 in the complex structure is remarkably different from that in the uncomplexed structure, although the participation of Arg359 in the catalytic reaction is not clear based on the present structural model. PLP leans slightly toward His123. In addition, Lys226 flips by about 120° around its Cγ-Cδ bond to form hydrogen bonds with the O3′ atom (2.7 Å) of the pyridine ring of PLP and with the Nε2 atom (2.5 Å) of Gln203. Gln203, which is hydrogen-bonded to the O3′ atom of the pyridine ring in the uncomplexed structure, is moved toward His207 so that the hydrogen bond with the O3′ atom can be broken in the PG complex (Fig. 2b). The interaction between Gln203 and Lys226 may favor the formation of the external aldimine by stabilizing the PLP-unligated Lys226 through the formation of the hydrogen bond to Nε2 of Gln203. The formation of this hydrogen bond may keep the free Nε-amino group of Lys226 in the unprotonated form, which is necessary for the base to accept the Cα proton of the substrate. Gln203 in CsdB is completely conserved in NifS/IscS homologs (*24*). In the PG complex, a new hydrogen bond is formed between Oε1 of Gln203 and Nε2 of His207. Nδ1 of His207 is hydrogen-bonded to the side-chain carboxylate of Glu306, which is hydrogen-bonded to the amino nitrogen of Met384, resulting in a hydrogen-bond network (PLP-Lys226-Gln-203-His207-Gln306-Met384) ranging from PLP to Met384. The closest proximity of the Cα atom of the substrate analog PG to the enzyme base is observed at Nε of Lys226 with a distance of approximately 5.1 Å. Lys226 is the only residue that is positioned appropriately to accept the Cα proton from the substrate. Therefore, it is likely that the deprotonated Nε of Lys226 abstracts the Cα proton from the substrate after formation of the external aldimine.

Mutagenesis Study of His55, His123, and Arg379 Located around Substrate-PLP—We have noted that His55, His123, and Arg379 are possibly involved in the catalytic reaction of CsdB. The structure of the CsdB-PG complex suggests that these residues must be located around the substrate-PLP site. Accordingly, we used site-dericted mutagenesis to replace each of His55, His123, and Arg379 with Ala to produce the mutants H55A, H123A, and R379A, respectively.

The activity of the H55A mutant toward both L-selenocysteine and L-cysteine was not decreased by the mutation.

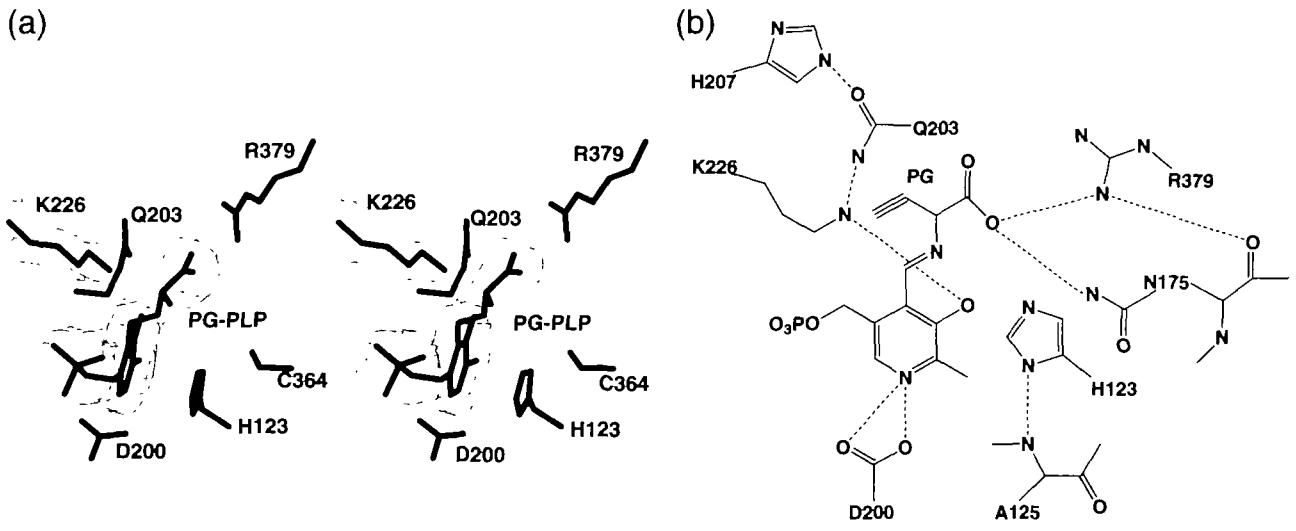

Fig. 2. **The CsdB-PG complex.** (a) A stereoview of the $2F_o–F_c$ map calculated at 2.8 Å resolution and contoured at 1.0 σ. The Cγ atom of PG is not shown in the figure because the model lacks the atom. The figure was generated with the program BOBSCRIPT (*28*). (b) Schematic representation of polar interactions in the CsdB-PG complex. Hydrogen atoms and charges are not shown in the figure because the protonation states of all species are not known. Presumed hydrogen bonds are indicated by dashed lines between atoms separated by less than 3.6 Å.

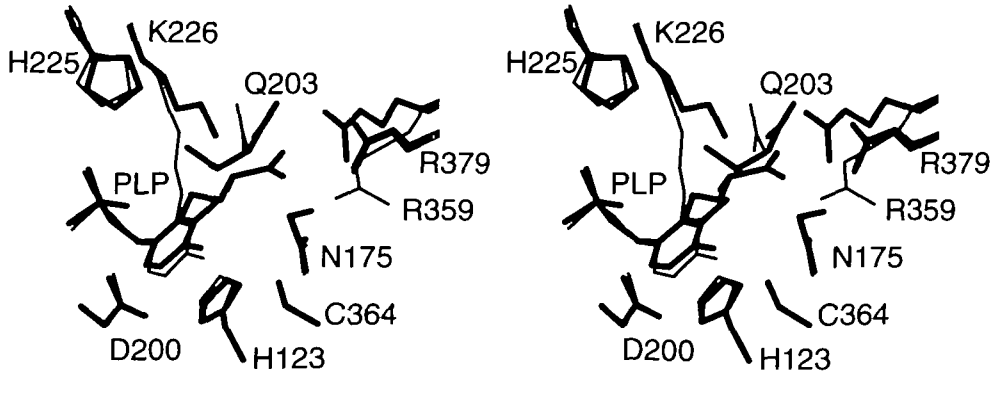

Fig. 3. **Stereo plot showing the superposition of the active site of the CsdB-PG complex (thicker lines) on that of the uncomplexed CsdB (thinner lines).** The figure was generated by MOLSCRIPT (*29*).

Although, in our previous paper, we hypothesized that His55, which projects from the other subunit in the dimer, is a putative recognition residue for the side chain of the substrate (*16*), His55 is not essential for catalysis.

The H123A mutant enzyme exhibits a decreased specific activity (0.050 unit/mg toward L-selenocysteine), which is less than 1% of the specific activity of the wild-type CsdB. Thus, His123 is important for catalysis. The absorption spectrum of the H123A enzyme is different from that of the wild-type enzyme. The absorption peak at 420 nm, which is due to an internal aldimine linkage between Lys226 and PLP, is significantly decreased in H123A, indicating that His123 may contribute to stabilizing PLP in the active site by a plane–plane interaction between the imidazole ring of His123 and the pyridine ring of PLP.

The R379A mutant enzyme showed a significant loss of activity toward L-selenocysteine (< 0.17% of that of the wild-type). As Arg379 interacts with the α-carboxyl group of PG, as described above, this residue probably defines the position of the substrate during catalysis. Thus, Arg379 is essential for the catalytic activity of CsdB.

Structural Comparison with tmNifS—CsdB and tmNifS share 23% sequence identity based on a structure-derived sequence alignment (Fig. 4). The structure of tmNifS (PDB # 1EG5) can be superimposed on that of the CsdB-PG complex with an average rms deviation of 1.5 Å over 319 Cα atoms, which is similar to the 1.5 Å between tmNifS and the uncomplexed CsdB. The folding of the large domain in the subunit is highly conserved between both structures, and the variable residues are largely confined to the surface of the subunit. The largest main-chain differences map the two regions that form the β-hairpin loop (residues 255–271) and the extended lobe (residues 362–375) anchoring the catalytic Cys364 (Fig. 5). Kaiser *et al.* reported that the active-site loop (Ser321–Ser332) bearing the putative active Cys324 in tmNifS is disordered, indicating that the loop is highly flexible (*19*). On the other hand, we observed clear electron density for the extended lobe of CsdB and determined the exact location of Cys364 in both the substrate-free enzyme and the PG-complexed enzyme. The interaction between the extended lobe in one subunit of the dimer and the β-hairpin loop in the other subunit is the most remarkable structural feature in CsdB. On the other hand, the β-hairpin loop, which makes up one side of the active site, is deleted in tmNifS. In contrast to this deletion, 11 residues are inserted between Asp336 and Ala348 in the region of tmNifS corresponding to the extended lobe of CsdB (Fig. 4). Therefore, the extended lobe containing the active Cys residue seems to be larger and much more extended in tmNifS than in CsdB, resulting in the enhancement in the flexibility of the region in tmNifS.

Does the Non-Flexible Extended Lobe Restrict the Cysteine Desulfurase Activity of CsdB?—We previously characterized the properties of three NifS homologs from *E. coli*

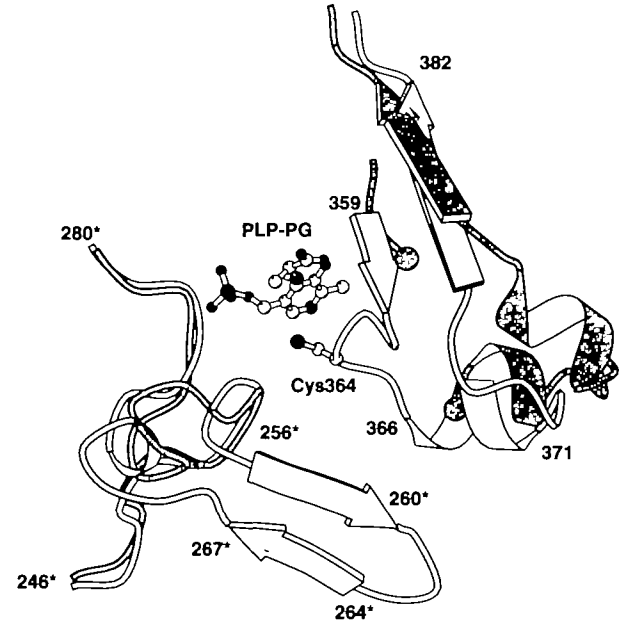

Fig. 5. **Superposition of the structure of the extended lobe of the CsdB-PG complex on that of tmNifS, showing the regions in which the structures differ markedly between CsdB and tmNifS.** The Cα trace of CsdB is in white and that of tmNifS (PDB accession number, 1EG5) in gray. The catalytic Cys364 and the PLP-PG moiety in CsdB are depicted as ball-and-stick models. Residue numbers are shown for CsdB. The Cα atoms of Thr220 and His333 in tmNifS, which encompass the disordered region, are depicted as balls. The figure was drawn with the program MOLSCRIPT (*29*).

Fig. 4. **Structure-based sequence alignment of CsdB and tmNifS.** Identical residues are marked by asterisks. Hyphens in the sequences represent gaps in the alignment. Residues not present in the coordinate files are denoted by small letters. Sequence numbers and secondary structural elements of CsdB are shown above the alignment. α-Helix regions are denoted by white bars and β-strand regions by horizontal arrows. The regions showing markedly different structures between CsdB and tmNifS are shaded on the alignment. The catalytic Cys residue is denoted by a vertical arrow.

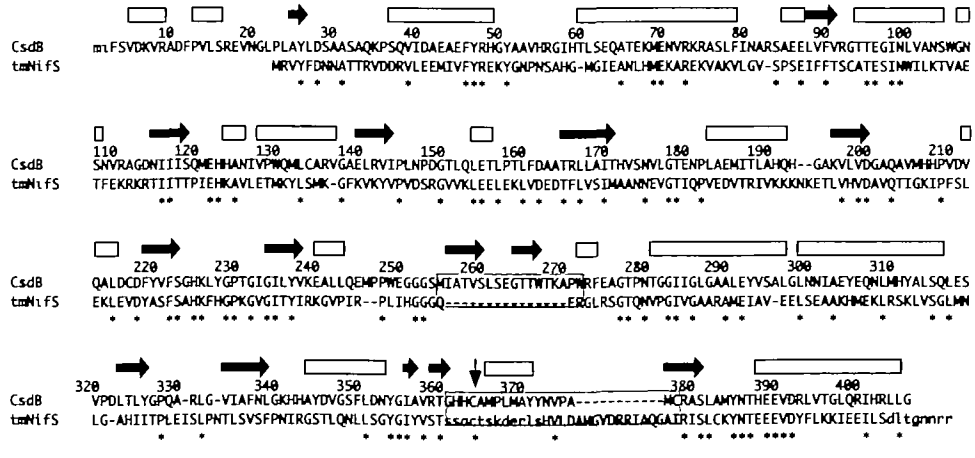

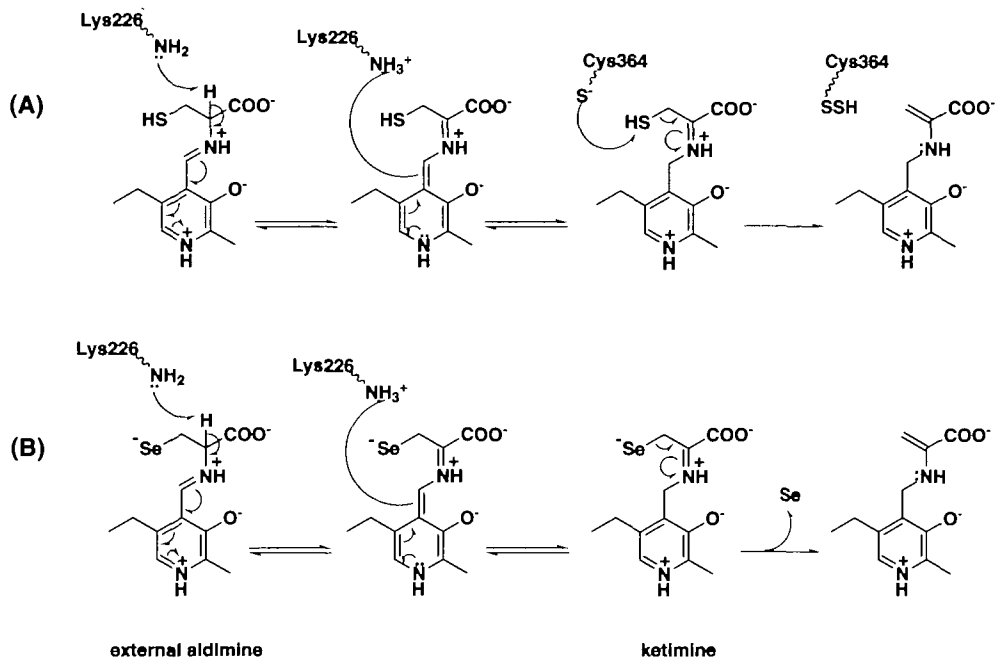

Scheme 1. **Proposed reaction mechanisms for cysteine desulfuration (A) and selenocysteine deselenation (B) catalyzed by CsdB.** The sulfhydryl group of L-cysteine is protonated, whereas the selenohydryl group of L-selenocysteine is deprotonated under the reaction conditions at pH 7.4. The desulfuration of L-cysteine requires nucleophilic attack by Cys364. In contrast, selenium is released spontaneously from the ketimine intermediate.

and showed replacing the conserved Cys of each enzyme with Ala completely abolished the activity of the enzymes toward L-cysteine, whereas the activity toward L-selenocysteine was less affected (*15*). Thus, we have proposed that the reaction mechanism of the enzymes with L-cysteine is different from that with L-selenocysteine (Scheme 1). According to the proposed reaction mechanism, the spatially precise positioning of the active-residue Cys is crucial for the cysteine desulfuration catalyzed by CsdB and tmNifS (*14, 15, 19*). In the previous paper, we discussed the putative binding mode of the substrate L-selenocysteine to CsdB by creating the docking model of the selenocysteine-CsdB complex based on the crystal structures of complexes of aspartate aminotransferase and phosphoserine aminotransferase with their substrate analogs (*25–27*). A discrepancy in the model is that the selenium at the γ-position of the cysteine substrate is located about 5 Å apart from the side chain of Cys364. This distance is too long for a direct interaction. Therefore, we wonder whether the Cys364 residue located on the extended lobe moves upon substrate binding so that the sulfhydryl group of Cys364 can perform the nucleophilic attack on the γ-position of the cysteine substrate. However, the Cys364 residue in the present CsdB-PG complex superimposes completely on that in the uncomplexed CsdB, implying the positional preservation of the Cys residue in both forms. In the CsdB-PG external aldimine complex, the distance between the presumptive γ atom of the substrate and Sγ of Cys364 is 4.8 Å. This distance is still too long for a direct interaction between them (Fig. 5). In order for Cys364 to act as the nucleophile attacking the sulfhydryl group of the substrate L-cysteine, the Sγ atom of Cys364 must get closer to the substrate-PLP intermediate during catalysis. As mentioned above, the extended lobe of CsdB is much shorter than that of tmNifS and seems to be fixed by interaction with the β-hairpin. In contrast, tmNifS has a presumably longer and more flexible extended lobe and lacks the β-hairpin structure, which possibly makes the enzyme much more reactive toward L-cysteine. Therefore, the low cysteine-desulfurase activity of CsdB is likely due to inadequate positioning of Cys364 brought about by the inefficient movement of the extended lobe. This possibly enables the enzyme to discriminate between selenium and sulfur.

REFERENCES

1. Zheng, L., White, R.H., Cash, V.L., Jack, R.F., and Dean, D.R. (1993) Cysteine desulfurase activity indicates a role for NIFS in metallocluster biosynthesis. *Proc. Natl. Acad. Sci. USA* **90**, 2754–2758
2. Esaki, N., Nakamura, T., Tanaka, H., and Soda, K. (1982) Selenocysteine lyase, a novel enzyme that specifically acts on selenocysteine. Mammalian distribution and purification and properties of pig liver enzyme. *J. Biol. Chem.* **257**, 4386–4391
3. Zheng, L., Cash, V.L., Flint, D.H., and Dean, D.R. (1998) Assembly of iron-sulfur clusters. Identification of an *iscSUA-hscBA-fdx* gene cluster from *Azotobacter vinelandii*. *J. Biol. Chem.* **273**, 13264–13272
4. Schwartz, C.J., Djaman, O., Imlay, J.A., and Kiley, P.J. (2000) The cysteine desulfurase, IscS, has a major role in *in vivo* Fe-S cluster formation in *Escherichia coli*. *Proc. Natl. Acad. Sci. USA* **97**, 9009–9014
5. Kambampati, R. and Lauhon, C.T. (1999) IscS is a sulfurtransferase for the *in vitro* biosynthesis of 4-thiouridine in *Escherichia coli* tRNA. *Biochemistry* **38**, 16561–16568
6. Lauhon, C.T. and Kambampati, R. (2000) The *iscS* gene in *Escherichia coli* is required for the biosynthesis of 4-thiouridine, thiamin, and NAD. *J. Biol. Chem.* **275**, 20096–20103
7. Kiyasu, T., Asakura, A., Nagahashi, Y., and Hoshino, T. (2000) Contribution of cysteine desulfurase (NifS protein) to the biotin synthase reaction of *Escherichia coli*. *J. Bacteriol.* **182**, 2879–2885
8. Zheng, L., White, R.H., Cash, V.L., and Dean, D.R. (1994) Mechanism for the desulfurization of L-cysteine catalyzed by the *nifS* gene product. *Biochemistry* **33**, 4714–4720
9. Mihara, H., Kurihara, T., Watanabe, T., Yoshimura, T., and Esaki, N. (2000) cDNA cloning, purification, and characterization of mouse liver selenocysteine lyase. Candidate for sele-

nium delivery protein in selenoprotein synthesis. *J. Biol. Chem.* **275**, 6195–6200
10. Neuhier, B. and Böck, A. (2000) On the mechanism of selenium tolerance in selenium-accumulating plants. Purification and characterization of a specific selenocysteine methyltransferase from cultured cells of *Astragalus bisculatus*. *Eur. J. Biochem.* **239**, 235–238
11. Stadtman, T.C. (1979) Some selenium-dependent biochemical processes. *Adv. Enzymol. Relat. Areas Mol. Biol.* **48**, 1–28
12. Stadtman, T.C. (1990) Selenium biochemistry. *Annu. Rev. Biochem.* **59**, 111–127
13. Heider, J. and Böck, A. (1993) Selenium metabolism in microorganisms. *Adv. Microbial. Physiol.* **35**, 71–109
14. Mihara, H., Maeda, M., Fujii, T., Kurihara, T., Hata, Y., and Esaki, N. (1999) A *nifS*-like gene, *csdB*, encodes an *Escherichia coli* counterpart of mammalian selenocysteine lyase. Gene cloning, purification, characterization and preliminary x-ray crystallographic studies. *J. Biol. Chem.* **274**, 14768–14772
15. Mihara, H., Kurihara, T., Yoshimura, T., and Esaki, N. (2000) Kinetic and mutational studies of three NifS homologs from *Escherichia coli*. Mechanistic difference between L-cysteine desulfurase and L-selenocysteine lyase reactions. *J. Biochem.* **127**, 559–567
16. Fujii, T., Maeda, M., Mihara, H., Kurihara, T., Esaki, N., and Hata, Y. (2000) Structure of a NifS homologue. X-ray structure analysis of CsdB, an *Escherichia coli* counterpart of mammalian selenocysteine lyase. *Biochemistry* **39**, 1263–1273
17. Mehta, P.K. and Christen, P. (1993) Homology of pyridoxal-5′-phosphate-dependent aminotransferases with the *cobC* (cobalamin synthesis), *nifS* (nitrogen fixation), *pabC* (*p*-aminobenzoate synthesis) and *malY* (abolishing endogenous induction of the maltose system) gene products. *Eur. J. Biochem.* **211**, 373–376
18. Alexander, F.W., Sandmeier, E., Mehta, P.K., and Christen, P. (1994) Evolutionary relationships among pyridoxal-5′-phosphate-dependent enzymes. Regio-specific alpha, beta and gamma families. *Eur. J. Biochem* **219**, 953–960
19. Kaiser, J.T., Clausen, T., Bourenkow, G.P., Bartunik, H.D., Steinbacher, S., and Huber, R. (2000) Crystal structure of a NifS-like protein from *Thermotoga maritima*. Implications for iron sulphur cluster assembly. *J. Mol. Biol.* **297**, 451–464
20. Brünger, A.T., Adams, P.D., Clore, G.M., DeLano, W.L., Gros, P., Grosse-Kunstleve, R.W., Jiang, J.S., Kuszewski, J., Nilges, M., Pannu, N.S., Read, R.J., Rice, L.M., Simonson, T., and Warren, G.L. (1998) Crystallography and NMR system. A new software suite for macromolecular structure determination. *Acta Crystallogr. D* **54**, 905–921
21. Cambillau, C. (1992) *Turbo-FRODO, version 5.02*, BioGraphics, Marseille, France
22. Ito, W., Ishiguro, H., and Kurosawa, Y. (1991) A general method for introducing a series of mutations into cloned DNA using the polymerase chain reaction. *Gene* **102**, 67–70
23. Laskowski, R.A., McArthur, M.W., Moss, D.S., and Thornton, J.M. (1993) PROCHECK: a programe to check the stereochemical quality of protein structures. *J. Appl. Crystallogr.* **26**, 283–291
24. Mihara, H., Kurihara, T., Yoshimura, T., Soda, K., and Esaki, N. (1997) Cysteine sulfinate desulfinase, a NIFS-like protein of *Escherichia coli* with selenocysteine lyase and cysteine desulfurase activities. Gene cloning, purification, and characterization of a novel pyridoxal enzyme. *J. Biol. Chem.* **272**, 22417–22424
25. Jäger, J., Moser, M., Sauder, U., and Jansonius, J.N. (1994) Crystal structures of *Escherichia coli* aspartate aminotransferase in two conformations. Comparison of an unliganded open and two liganded closed forms. *J. Mol. Biol.* **239**, 285–305
26. Okamoto, A., Higuchi, T., Hirotsu, K., Kuramitsu, S., and Kagamiyama, H. (1994) X-ray crystallographic study of pyridoxal 5′-phosphate-type aspartate aminotransferases from *Escherichia coli* in open and closed form. *J. Biochem.* **116**, 95–107
27. Hester, G., Stark, W., Moser, M., Kallen, J., Markovic-Housley, Z., and Jansonius, J.N. (1999) Crystal structure of phosphoserine aminotransferase from *Escherichia coli* at 2.3 Å resolution. Comparison of the unligated enzyme and a complex with α-methyl-L-glutamate. *J. Mol. Biol.* **286**, 829–850
28. Esnouf, R.M. (1997) An extensively modified version of MolScript that includes greatly enhanced coloring capabilities. *J. Mol. Graph. Model.* **15**, 132–134
29. Kraulis, P.J. (1991) MOLSCRIPT: a program to produce both detailed and schematic plots of protein structures. *J. Appl. Crystallog.* **24**, 946–950